PAPER • **OPEN ACCESS**

Simulation Study of the Influence of Ultrasonic Energy Flow Density on the Properties of Zirconium-based Amorphous Alloys at Room Temperature

To cite this article: Fangping Liu *et al* 2019 *IOP Conf. Ser.: Mater. Sci. Eng.* **490** 052017

Simulation Study of the Influence of Ultrasonic Energy Flow Density on the Properties of Zirconium-based Amorphous Alloys at Room Temperature

Fangping Liu, Xiao Liu and Yan Lou*

School of Mechatronics and Control Engineering, Shenzhen University, Guangdong, China

*Corresponding author e-mail: susanlou121@163.com

Abstract. Zr-based amorphous alloy was firstly pretreated with ultrasonic-assisted vibration microcompression at different amplitudes and frequencies, and then the samples were compressed till fracture. The process were simulated by using the finite element analysis software ABAQUS. The reliability of the finite element model was validated by comparing the simulation and experimental results. The effect of the energy flow density on the deformation behavior of Zr-based amorphous alloy at room temperature was studied at ultrasonic amplitudes of 0, 19, 27, 36, and 43 μm and frequencies of 20, 25, 30, and 35 kHz. Results showed that with the increasing of ultrasonic amplitude and frequency, the elastic modulus decreased, and the equivalent stress distributions were more uniform, and the formability increased. This was due to the temperature rise and increasing of the free volume concentration of the compressed samples caused by the ultrasonic vibration. However, it is found that the formability of amorphous alloy decreased with the increase of ultrasonic energy flow density when the density increased to approximately $I = 9.41\times10^{8}$ W·m^{-2}. The phenomenon was because the temperature rise caused by the ultrasonic heating effect exceeded the termination crystallization temperature of amorphous alloy, and fully crystallizing reaction occurred.

1. Introduction

Amorphous alloy is a new type of material with excellent properties and wide application prospect. The Zr-based amorphous alloy has high elasticity, high hardness,excellent corrosion resistance, and superplastic forming properties in the supercooled liquid region. However, the brittleness at room temperature limits the application of this alloy. Thus, an ultrasonic-assisted vibration process is introduced to improve the plastic formability and thus enhance the structure and performance of the alloy. F. Blala et al. first introduced the effect of ultrasonic vibration on plastic processing in 1955 by performing tensile tests on a single crystal zinc. Ultrasonic vibration significantly reduces the yield and flow stresses of a specimen. This phenomenon is called the softening effect, also known as the Blala effect. In 2007, SAAA.Mousavi et al. [1] superimposed ultrasonic vibration during microextrusion. Results showed that the extrusion force and flow stress can be reduced and that increasing the amplitude can significantly reduce the extrusion force. Y.Daud et al. [2] applied ultrasonic vibration to the tensile and extrusion processes of aluminum alloy and found that the vibration sample produces a softening effect and that the friction between the contact surfaces of the

mold is reduced. Results of tests and finite element simulation proved that a reduction in flow stress during ultrasonic-assisted vibration process from a combination of acoustic softening, stress superposition, and surface effects. In 2009, Hung et al. [3] performed ultrasound-assisted annular extrusion tests and found that extrusion decreases the forming force and increases the temperature. In 2013, T.Wen et al. [4] superimposed ultrasonic vibration on the upsetting compression of Mg alloys. Results showed that the yield strength and flow stress of the material are decreased, and the reduction range is related to the material properties. When the vibration energy is large, hardening phenomenon occurs, that is, the softening of the weak vibration and the hardening phenomenon of the strong vibration. The vibration helps to improve the quality of the compressed surface. In 2016, C.X.Chen et al. [5] used ABAQUS software to simulate the ultrasonic-assisted microextrusion of T2 copper parts under different vibration modes. They found that that the applied vibration energy can obtain a uniform superimposed stress field and equivalent stress. In 2017, Li et al. [6] introduced ultrasonic vibration into the deformation at supercooled liquid region of amorphous and a high-temperature uniaxial compression test was performed on Zr-based amorphous alloy. Results showed that ultrasonic vibration can reduce the flow stress of the amorphous alloy. Moreover, the greater the input power is, the more favorable the deformation of the amorphous alloy will be.

Finite element simulation has been widely used in multidisciplinary, macroscopic, and microscopic aspects because it can manifest the microstructure evolution and mechanical performance changes of a material . In the present study, the ultrasonic-assisted microcompression of Zr-based amorphous alloys at different amplitudes and frequencies was firstly conducted and then these samples were quasi-static compressed at room temperature. The processes were simulated by using ABAQUS finite element software. The performance of the alloy was then evaluated to investigate the relationship of the microstructure, properties, and vibration load of the Zr-based amorphous alloy.

2. Experimental procedures

2.1. Sample preparation

An amorphous alloy $Zr_{52.5}Cu_{17.9}Ni_{14.6}Al_{10}Ti_5$ (atomic percentage) was used in the present study. Raw material was prepared using Zr, Cu, Ni, Al, and Ti with a purity of 99.9% as nominal compositions, and then an electric arc furnace was used to smelt the mother alloy. Amorphous rod-shaped specimens were obtained by a copper mold suction casting method. We used a numerical control wire cutting method to process the sample. The bottom surfaces of φ2×4 mm cylindrical specimens were polished to ensure parallelism and perpendicular to the loading axis.

2.2. Ultrasonic-assisted vibration treatment

Before the compression fracture tests, the samples were pretreated with ultrasonic-assisted vibration. The treatment was conducted using a ultrasonic-assisted vibration compression testing platform (Fig 1) consisting of an ultrasonic generator at a frequency of 20 kHz, a transducer and a horn. The horn was also used as an indenter and embedded in a universal tensile tester . Given the ultrasonic vibration , the clamp adopted the upper and lower splint structures. The sample was positioned and fixed through the fixing holes of the fixing plate. The upper splint was pressed to prevent misalignment during vibration. The upper and lower splints were connected by fastening screws.

The specimens were subjected to vibrations with amplitudes of 0, 19, 27, 36, and 43 μm. The amplitude of 0 μm means without ultrasonic vibration. The strain rate was 0.005/s, and then the specimen was compressed by 2% within the elastic limit and then unloaded.

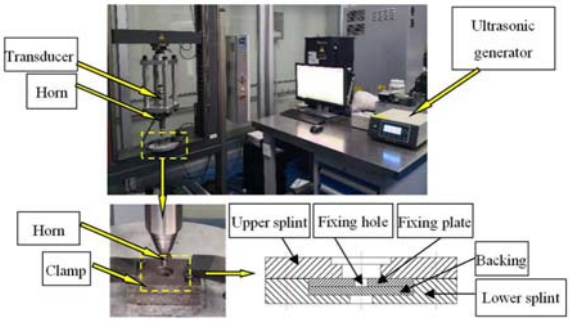

Figure 1. Ultrasonic-assisted vibration compression test platform.

2.3. Compression test

The stress-strain curves for the above samples were obtained by performing quasi-static compression fracture tests on the samples with a strain rate of 0.005/s, conducted on a universal tensile tester (Zwick Z050) (Fig 2).

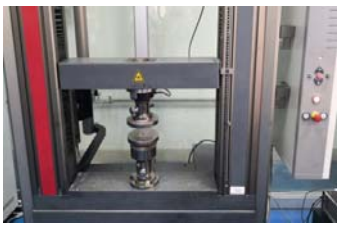

Figure 2. Zwick Z050 compression testing machine.

3. Finite element modelling

The finite element model of the compression test with a sample of φ2× 4 mm was set up. The true stress-strain curve of the Zr-based amorphous alloy was obtained from the experimental results. The ABAQUS finite element analysis software was used to simulate the ultrasonic-assisted vibration microcompression pretreated process and the quasi-static compression fracture process. In the simulation analysis, the frequency of ultrasonic vibration was set to *f* kHz, and the amplitude was set to *A* μm. Ultrasonic loading was achieved by adding a cosine-deflected velocity to the indenter.

During the ultrasonic-assisted vibration compression process, a high-speed nonlinear contact behavior was observed at the contact surface between the indenter and the specimen. Therefore, the model was equivalently treated to simulate the actual complex contact behavior. The sampling axis symmetry model was used to calculate the compression process, to simplify the modeling and solving process and save computer resources. 2D unit CAX4I was used for simulation.

The material parameters used in the model are: modulus of elasticity of 82 GPa, Poisson's ratio of 0.34, density of 6.49 g/cm^3, and the flow stress data were inputted according to the data obtained by the above experiments. The indenter was defined as rigid, and the sample was defined as elastoplastic. The bottom surface of the sample was set to be fixed. To ensure convergence, we used three analysis steps. The first analysis step was slightly in contact. The second analysis step was the ultrasonic-assisted vibration microcompression to 2%, and then unloaded. The third analysis step was directly quasi-static compressed fracture. As the entire sample was uniformly compressed without the appearance of a drum, accurate analysis results will be obtained.

Fig 3 shows the comparison of the simulated and experimental flow stress at strain rate of 0.005/s for quasi-static fracture compression, and ultrasonic-assisted vibration preconditioning at frequency of 20 kHz and different amplitudes. The solid line indicates the experimental values and the dashed line indicates the simulated ones. It can be found that the error was only approximately 3%, indicating that the established simulation model is reliable.

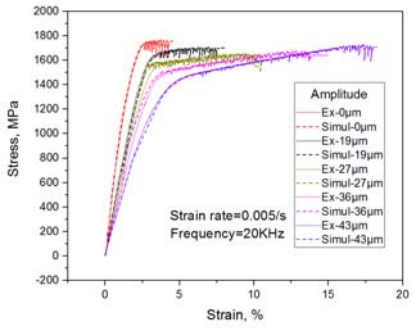

Figure 3. Comparison of the simulated and experimental flow stress at strain rate of 0.005/s for quasi-static fracture compression, and ultrasonic-assisted vibration preconditioning at frequency of 20 kHz and different amplitudes .

To save experiment cost and time, deformation behavior of the Zr-based amorphous alloy at different frequencies and amplitudes was analyzed with the verified FEM model. The simulation testing scheme was shown in Table 1.

Table 1. Ultrasonic-assisted vibration testing scheme for FEM simulation.

Numble	Amplitude (μm)	Frequency (kHz)	Fixed condition
1	19	20	According to the standard compression model, the elastic modulus is 82 GPa, the Poisson's ratio is 0.34, and the density is 6.49 g/cm^3.
2	19	25	
3	19	30	
4	19	35	
5	27	20	
6	27	25	
7	27	30	
8	27	35	
9	36	20	
10	36	25	
11	36	30	
12	36	35	
13	43	20	
14	43	25	
15	43	30	
16	43	35	

4. Simulation results

According to testing plans 1-16, the parameters were set in order, and the stress-strain curve of the quasi-static compression fracture of the samples after the different ultrasonic amplitude pretreatments was obtained (Fig 4).

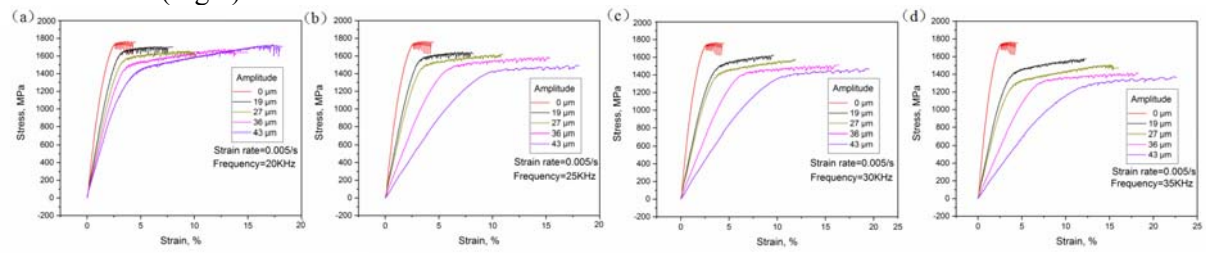

Figure 4. Stress-strain curve of compression fracture of the specimen after pretreatment with different ultrasonic amplitudes of (a) 20, (b) 25, (c) 30, and (d) 35 kHz.

The simulated equivalent stress and strain contour diagrams are shown in Table 2. The vibration frequency of 30 kHz and the amplitudes of 0, 19, 27, 36, and 43 μm were applied to the sample treated with ultrasonic vibration. The strain rate of quasi-static compression fracture was 0.005/s.

Table 2. Equivalent stress and strain contour diagrams of quasi-static compressive fracture of the specimens after pretreated with ultrasonic vibration of a frequency of 30 kHz and different amplitudes.

A/μm	0	19	27	36	43
σ	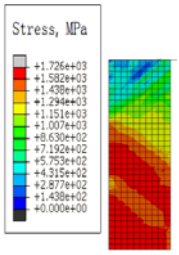	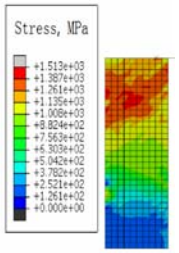	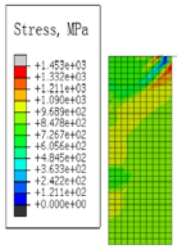	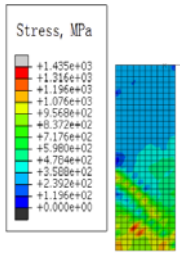	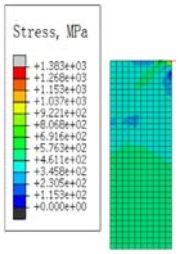
ε	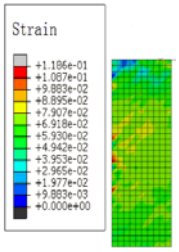	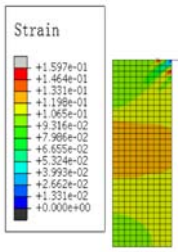	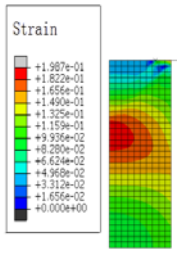	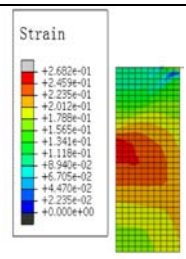	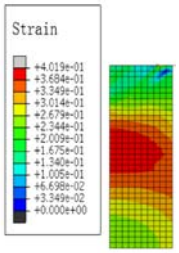

As shown in Table 2, the maximum equivalent stress of the sample decreased after the ultrasonic-assisted vibration pretreatment, and the distribution of equivalent stress was also more uniform. The maximum equivalent stress decreased with the increase in amplitude. As shown in the equivalent strain contour diagram, the maximum equivalent strain of the sample after ultrasonic-assisted vibration treated increased with increasing amplitude, indicating that increasing the amplitude can effectively improve the formability of the specimen. Y.Hiki also got the similar results [7].

To consider the effect of vibration frequency on properties of amorphous alloy, the stress-strain curves the quasi-static compression fracture of the samples after the treatment with different ultrasonic vibration frequencies were obtained in Fig 5 according to testing plans 1-16.

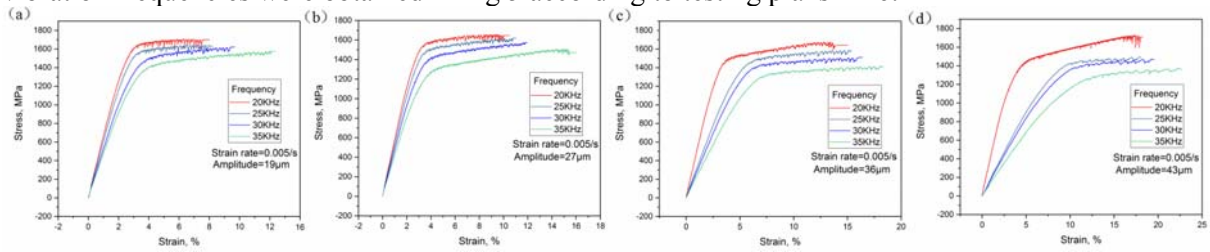

Figure 5. Stress-strain curve of compression fracture of the specimen after pretreatment with different ultrasonic vibration amplitudes of (a) 19, (b) 27, (c) 36, and (d) 43 μm.

Table 3 illustrates the equivalent stress and strain contour diagrams of the quasi-static compression fracture of the samples pretreated at vibration frequencies of 20, 25, 30, and 35 kHz and an amplitude of 19 μm.

Table 3. Equivalent stress and strain contour diagrams of quasi-static compressive fracture of the specimens after pretreated with ultrasonic vibration of an amplitude of 19μm and different frequencies.

f/kHz	20	25	30	35
σ	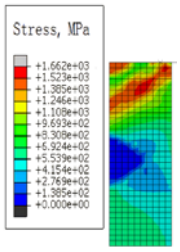	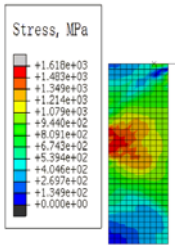	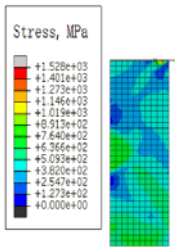	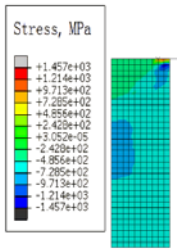
ε	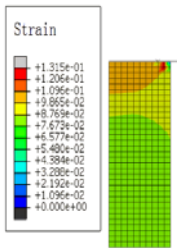	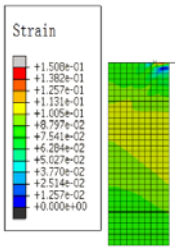	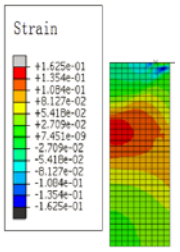	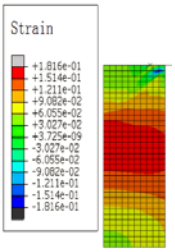

It can be found in Table 3 that the maximum equivalent stress decreased and the maximum equivalent strain of the sample increased with the increase in frequency. It means that increasing the vibration frequency can effectively increase the formability of the Zr-based amorphous alloy.

According to the variations of the slopes of the stress-strain curves in Figs 4 and 5, the elastic modulus of Zr-based amorphous alloy decreased as the amplitude or frequency increased. This phenomenon is due to the fact that the plastic deformation of amorphous alloys is mainly accomplished by the sliding, nucleation, and expansion of shear bands [8]. D.S.Sanditov [9] believed that amorphous alloys contain free volume, the presence of these free volumes increases the interatomic distance and reduces the interaction forces. The ultrasonic-assisted vibration loading could increase the free volumes concentration [10] so as to cause the sample to generate a softening phenomenon. The softening rate increased with the increase of ultrasonic amplitude or frequency. The energy of the ultrasonic wave increases with increasing amplitude or frequency. After the sample absorbed the energy of the ultrasonic wave, it transmitted the longitudinal vibration. In the sample, part of the energy was absorbed by the atoms inside the sample. Moreover, the activity of the atoms increased, and the temperature of the sample increased, thereby increasing the free volume concentration of the amorphous alloy. This phenomenon led to the decrease of elastic modulus [11] and deformation resistance, thereby improved the forming ability.

5. Quantitative characterization of energy flow and formability

When ultrasound propagates in a solid medium, part of the energy will be absorbed, and the absorbed energy will be converted into thermal energy, which will increase the internal temperature of the solid medium. Through the analysis of the heat transfer absorption mechanism, the heat absorption coefficient of the longitudinal wave propagating in the cylindrical rod as follows [12]:

$$\alpha_l = \frac{w^2}{2\rho C_L^{\,3}}\left[\left(\frac{4}{3}\mu' + \lambda'\right) + \frac{k_t T \alpha_t C_t^{\,2}}{C_p^{\,2}}\left(1 - \frac{4C_t^{\,2}}{3C_L^{\,2}}\right)^2\right] \tag{1}$$

where w is the angular frequency, ρ is the material density, C_L is the propagation speed of the longitudinal wave in the medium, C_t is the propagation speed of the transverse wave in the medium, μ' is the imaginary part of the first Raman coefficient, λ' is the imaginary part of the second Raman coefficient, k_t is the thermal conductivity, α_t is the thermal diffusivity, and C_t is the constant pressure heat capacity.

The longitudinal wave speed of ultrasonic C_L can be described as follows [12]:

$$C_L = \sqrt{\frac{E(1-\sigma)}{\rho(1+\sigma)(1-2\sigma)}} \tag{2}$$

Meanwhile, the shear wave speed of ultrasonic C_t can be described as follows:

$$C_t = \sqrt{\frac{E}{2\rho(1+\sigma)}} \tag{3}$$

where E is the elastic modulus of the material, ρ is the material density , and σ is Poisson's ratio.

For Zr-based amorphous alloys, the parameters in Equations (2) and (3) are as follows [13]: $E = 82GP\text{a}$, $\sigma = 0.34$, $C_L = 4410m/s$, $C_\text{t} = 2171m/s$.

The parameters in Equation (1) are as follows [13]: $\rho = 6.49\text{g/cm}^3$, $\mu' = 35.3GP\text{a}$, $\lambda' = 94.5GP\text{a}$, $\text{k}_t = 16.7W\cdot m^{-1}K^{-1}$, $\alpha_t = 5.80\mu m\cdot m^{-1}K^{-1}$, and $C_p = 26.00J\cdot \text{mol}^{-1}K^{-1}$. Substituting all parameters into Equation (1) yields the heat absorption coefficient $\alpha_l = 0.200$.

Ultrasonic energy flow density *I* comprehensively reflects the vibration effect of ultrasonic waves. In the present study, energy flow density I and elongation δ were used to characterize the deformation behavior of amorphous alloy.

The ultrasonic energy flow density is obtained using the following formula [14]:

$$I = \frac{1}{2}\rho c w^2 A^2 \tag{4}$$

where ρ is the material density, $\rho = 6.49g/cm^3$, c is the speed at which the ultrasonic wave propagates in the medium, $c = \text{C}_\text{L} = 4410m/s$, w is the angular frequency, $w = 2\pi f$, and A is the ultrasonic amplitude.

Ultrasound frequencies of 20, 25, 30, and 35 kHz and amplitudes of 19, 27, 36, and 43 μm were substituted in Equation (4) to determine the energy flow density.

To characterize the quantitative relationship between the forming ability and the energy flow density, we defined the correlation function as follows:

$$\delta = aI^2 + bI + c \tag{5}$$

On the basis of the above mentioned calculation results, linear regression was performed using the principle of least squares, and the fitting function was obtained as follows:

$$\delta = (-8.23862\text{E}-18)\cdot I^2 + (1.50577\text{E}-8)\cdot I + 3.87442 \tag{6}$$

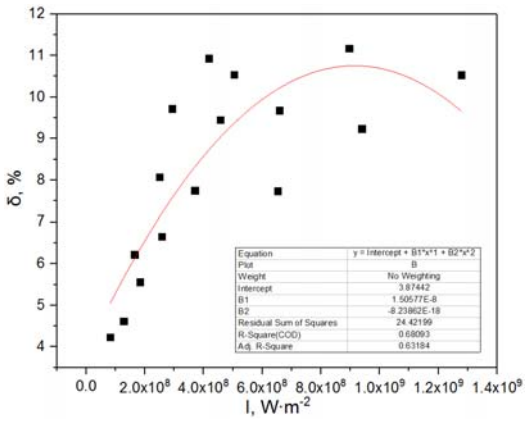

Figure 6. Relationship between energy flow density and formability.

Fig 6 shows the relationship between energy flow density and formability. It can be seen that the formability increased with the increase in energy flow density. However, when the energy flow density exceeded a certain value, the formability decreased continuously and ultrasonic hardening occurred. The inflection point coordinates of the curve were (9.41×10^8 , 10.75).

Due to high frequency and high amplitude ultrasonic vibration, the temperature of Zr-based amorphous alloy significantly increased during deformation. The deformation temperature increased with increasing frequency and amplitude. Therefore, effect of temperature rise on the deformation behavior of amorphous alloy should be explored.

Ultrasonic-induced temperature rise can be estimated using the following theoretical formula [14]:

$$\Delta T = \frac{a_l \cdot I}{4\rho C_p} \tag{7}$$

where a_l is the heat absorption coefficient of the amorphous alloy ($\alpha_l = 0.200$,), I is the ultrasonic energy flow density, ρ is the material density ($\rho = 6.49 g/cm^3$,), and C_p is the constant pressure heat capacity ($C_p = 26.00 J\cdot mol^{-1}K^{-1}$).

The energy flow density $I = 9.41\times10^8 W\cdot m^{-2}$ represented by the coordinates of the inflection point was substituted to Equation (4-7) to obtain a temperature rise of ΔT= 541.66 °C. The start crystallization temperature of Zr-based amorphous alloy was approximately 450 °C, and the termination temperature was approximately 530 °C [15]. The temperature rise caused by the ultrasonic heating effect at the inflection point exceeded the termination crystallization temperature. The occurrence of fully crystallization led to a decrease in formability.

6. Conclusions

1. Ultrasonic-assisted vibration loading pretreatment of Zr-based amorphous alloy specimens at room temperature result in ultrasonic softening. A part of the energy was absorbed by the internal atoms. The activity of the atom and the deformation temperature of the sample increased accordingly. The energy of the ultrasonic wave also increased with the increase of the amplitude or frequency leading to the increasing of the free volume concentration. Due to the decrease of the interaction force as the atomic distance increase, the elastic modulus and the deformation resistance decreased and the formability improved.

2. In a certain range, the forming ability of Zr-based amorphous alloy increased with the increase in energy flow density. However, when the energy flow density exceeds $I = 9.41\times10^8 W\cdot m^{-2}$, ultrasonic hardening occurred. The temperature rise caused by the ultrasonic thermal effect exceeded the termination crystallization temperature of the amorphous alloy, and the occurrence of fully crystallization led to a decrease in formability.

Acknowledgments

The authors gratefully acknowledge research support from the National Natural Science Foundation of China (Grant No.51675347), the National Natural Science Foundation of Guangdong Province (No. 2016A030313058), and the Science and Technology Project of Shenzhen (No. JCYJ20160308091758179).

References

[1] SAAA.Mousavi, H.Feizi, R.Madoliat, Investigations on the effects of ultrasonic vibrations in the extrusion process, J Mater Process Technol. 187-188(2007)657-661.

[2] Y.Daud, M.Lucas, Z.Huang, Modelling the effects of superimposed ultrasonic vibrations on tension and compression tests of aluminum, J Mater Process Technol. 186(2007)179-190.

[3] J.C.Hung, M.C.Chian, The Influence of Ultrasonic-Vibration on Double Backward-Extrusion of Aluminum Alloy,World Congress on Engi- neering, London, 2009, July 1-3. pp. 1814-1819.

[4] T.Wen, X.Chen, Effects of the Ultrasonic Vibration on the Plastic Deformation Behavior in the Compression Process of Light Alloys, Mechanical Science & Technology for Aerospace Engineering. 32(2013)221-224.
[5] C.X.Chen, G.C.Han, Z.Peng, H.R.Yang, X.Y.Wang, Ultrasonic-assisted micro-extrusion numerical simulation study. National Ultrasonic Processing Technology Symposium, Dalian,2016, October.pp. 21-23, 125-129.
[6] H.Li, Z.Z.Zheng, X.Wu, J.J.Li, Distortion of $Zr_{55}Cu_{30}Al_{10}Ni_5$ bulk amorphous alloy under ultrasonic vibration, China Mechanical Engineering. 28(2017)2514-2519.
[7] Y.Hiki, M.Tanahashi, S.Takeuchi, Temperature, frequency, and amplitude dependence of internal friction of metallic glass, Journal of Non-Crystalline Solids. 354 (10–11)(2008)994-1000.
[8] D.S.Sung, O.J.Kwon, E.Fleury, K.B.Kim, J.C.Lee, D.H.Kim, Y.C.Ki, Enhancement of the glass forming ability of Cu-Zr-A1 alloy by Ag addition, Metal Mater Int. 10(2004)575-579.
[9] D.S.Sanditov, Free volume of amorphous substances in the model of delocalized atoms, Doklady Physical Chemistry. 464(2015) 255-257.
[10] N.Li, X.Xu, Z.Zheng, L.Liu, Enhanced formability of a Zr-based bulk metallic glass in a supercooled liquid state by vibrational loading, Acta Materialia. 65(2014)400-411.
[11] S.V.Ketov, H.K.Nguyen, A.S.Trifonov, K.Nakajima, D.V.Louzguine, Huge reduction of Young's modulus near a shear band in metallic glass, Journal of Alloys & Compounds. 687(2016)221-226.
[12] O.V.Abramov, High-intensity ultrasonics: theory and industrial application, Kurnakov institute of general and inorganic chemistry, Moscow, 1998, pp. 80-124.
[13] A.Nayer,The Metals Databook, McGraw-Hill, New York, 1997.
[14] V.F.Humphrey, Ultrasound and matter-Physical interaction, Progress in Biophysics and Molecular Biology. 93(2007)195-211.
[15] H.Zong, L.Bian, J.Cheng, G.Cao, C.Kang, M.Li, Glass forming ability, thermal stability and elastic properties of Zr-Ti-Cu-Be-(Fe) bulk metallic glasses, Results in Physics. 6(2016)1157-1160.